中國機械工程學刊第四十三卷第一期第 11~19 頁(民國一百一十一年)
Journal of the Chinese Society of Mechanical Engineers, Vol.43, No.1, pp 11~19 (2022)

Deterioration Phenomena of a High Temperature PEM Fuel Cell with Bare SS304 Bipolar Plates

Chen-Yu Chen * and Chia-Hao Liang**

Keywords：fuel cell deterioration; high temperature proton exchange membrane fuel cell; metal bipolar plate; stainless steel.

ABSTRACT

The high temperature proton exchange membrane (HT-PEM) fuel cell using metal bipolar plates (BPs) can solve some challenges of traditional PEM fuel cells, including low CO tolerance and high BP cost. To improve its operating life, understanding the deterioration phenomena of the HT-PEM fuel cells using bare metal BPs is necessary. This work studies this fundamental subject and verifies the reasons for the cell deterioration. The experimental results indicate that the cell power with bare SS304 BPs decreases by about 53.5%, and the total cell resistance increases by about 92.5% after a continuous 384-h operation. The increase in the electrical resistance of the BPs due to formation of a passivation film on the SS304 surface is the major reason for the deterioration phenomena. Moreover, the cathodic BP after a continuous operation has a larger rugged surface area and a wider O and P elements distribution than the anodic BP, because of more produced water and more phosphoric acid leaks on the cathode side during operation, which causes more serious oxidation and corrosion problems. A stricter anti-corrosion criterion for the cathodic metal BP may be needed for this type of fuel cell.

INTRODUCTION

Recently, many environmental problems, such as global warming, extreme climate, acid rain, and an increase of particulate matter in the air, have been caused by burning fossil fuels. These problems affect the development of human civilization. Thus, the demand for cleaner energy technologies is increasing. However, most of the renewable energy sources, such as solar power and windy energy, currently face a challenge of unstable power output, and thus plenty of energy storage approaches have been proposed for overcoming this challenge. Power-to-hydrogen technologies and the power regeneration systems based on fuel cells are considered one of the practical solutions to the energy storage and electricity regeneration (Eveloy, 2018; Gondal, 2019). In addition to the practicability of energy storage, hydrogen and fuel cell systems also have other advantages, such as high efficiency, high reliability, good modulability, and being eco-friendly. As a result, in many developed countries, the fuel cell technology has been chosen as a focus of alternative energy development.

A high temperature proton exchange membrane (HT-PEM) fuel cell is usually operated at between 150-200 ^{o}C and is a very promising fuel cell system. The carbon monoxide tolerance of this type of fuel cell is high enough to tolerate 1-3% CO in H_2, and thus it is practical for reformate fuel cell systems. Moreover, its rejected heat has better recoverability due to higher operating temperature. Compared to a traditional proton exchange membrane (PEM) fuel cell, it is more suitable for stationary fuel cell systems with reformed H_2 supply sub-systems, because the H_2 purification sub-system for HT-PEM fuel cells is less critical than that for traditional PEM fuel cells.

The common type of electrolyte system for HT-PEM fuel cells is the acid doped polymer membrane. For the acid doped membranes, the major hydrogen proton transport is based on the hopping mechanism via hydrogen bonds between solvent molecules (Altaf et al., 2021), and thus water is not essential for fuel cell operation (Yusoff et al., 2020). As acid doped polymer membranes can work without water, they are able to operate at temperatures higher than 100 ^{o}C. Among all kind of proposed electrolyte systems for HT-PEM fuel cells, the H_3PO_4-doped polybenzimidazole (PBI)-based and the pyridine-based membranes (Charalampopoulos et

Paper Received July, 2021. Revised October, 2021. Accepted November, 2021. Author for Correspondence:Chen-Yu Chen.

* *Assistant Professor, Department of Mechanical and Energy Engineering, National Chiayi University, Chiayi City, Taiwan 60004, ROC.*

** *Department of Energy and Refrigerating Air-Conditioning Engineering, National Taipei University of Technology, Taipei, Taiwan 10608, ROC.*

al., 2020; Chen et al., 2020) are currently the two successful and commercially available systems. Their common points include high conductivity, good gas separability, good chemical stability at high temperature, good mechanical strength at high temperature and containing phosphoric acid (H_3PO_4).

It has been demonstrated that the PEM fuel cells can be applied in portable and stationary applications. However, some critical problems, including the costs associated with the noble metal catalyst and graphite bipolar plates (BPs) in the fuel cells, still need alternative solutions before the PEM fuel cells enter the commercial market (Moreno et al., 2015). Thus, applying stamped metal BPs instead of traditional graphite BPs in the PEM fuel cell stacks, which are usually produced by traditional milling methods, is considered a promising method to reduce the cost of the stacks. Moreover, using stamped BPs can reduce the weight, volume and the vibration-proof ability of the stack. Thus, the studies on the metal BPs for PEM fuel cells become attractive to researchers in recent years. The most common materials of present metal BPs are stainless steel (Hu et al., 2019; Song et al., 2020) because this material is well accessible. Some people as well proposed the BPs made of titanium or aluminum alloy (Shi et al., 2020; González-Gutiérrez et al., 2019) because of its better corrosion resistance or lower cost. Metal has the advantages of good mechanical stability, high thermal and electrical conductivity, and great fabrication formability. Nevertheless, the acid nature (pH value ranging between 2-3), humid environment and high temperature inside PEM fuel cells cause corrosion and dissolution problems. Thus, there are still many aspects that should be studied and improved for applying the metal BPs in PEM fuel cells.

According to the above introduction, one can understand that HT-PEM fuel cells are promising solid electrolyte fuel cells. In addition, using metal BPs is a future trend for PEM fuel cells. However, the research combining the HT- PEM fuel cell and metal BPs is still not common. This is because metal suffers from a corrosion problem in the acid environment. The operating temperature and the acid content in the membrane electrode assembly (MEA) of HT-PEM fuel cells are both higher than those of traditional PEM fuel cells. Thus, the corrosion problem of metal BPs is expected to be more serious than that in traditional PEM fuel cells, and is inferred to affect the available operational duration of HT-PEM fuel cells more significantly. Before proposing suitable and cost-efficient solutions to the reduced operational duration of this type of fuel cell, it is necessary to understand the performance deterioration mechanism of the HT-PEM fuel cells with metal BPs first.

The studies about the performance degradation of HT- PEM fuel cells have been presented by some researchers. For example, Qi and Buelte (2006) studied the relationship of the open circuit voltage, and the performance deterioration of PBI/H_3PO_4 fuel cells under 180ºC. They found that the Pt crystallite size on the cathode side became 4.3 times bigger as the cell was operated under the open circuit voltage for 244.5 h. Liu et al. (2006) mentioned that physical deterioration of membrane, agglomeration of both the anodic and cathodic catalysts, and H_3PO_4 leaching from the solid electrolyte were the main reasons for the performance drop of the HT-PEM fuel cells using H_3PO_4 doped PBI membrane. In 2006, the changes in the effective surface area of the catalyst and the high frequency resistance of a PBI/H_3PO_4 HT-PEM fuel cell with time were investigated by Hu et al. (2006, 2006). Their results indicated that cell performance drop was mainly due to the decrease of catalyst effective surface area because of sintering after a 500-h long-term experiment. Modestov et al. (2009) reported the results of a 780-h duration test of a PBI/H_3PO_4 MEA. A voltage decrease rate of 25 μV h^{-1} was obtained in the test and the growth of Pt size was inferred the major cause of the MEA deterioration. Oono et al. (2010) carried out a continuous durability test of the HT-PEM fuel cell with PBI/H_3PO_4 membranes at the temperatures ranging from 150 to 190◦C. They indicated that the performance drop in the early stage was caused by the catalyst aggregation. In the terminal stage, the performance degraded because of the depletion of H_3PO_4 in the membrane. Oono et al. (2012) studied the cell degradation mechanism of a HT-PEM fuel cell with PBI/H_3PO_4 MEAs. After a 17860-h operation, both the oxidation of the carbon support and the growth of the Pt particles were observed. They also found that the cell performance declined rapidly after 14000 h due to a decrease in the membrane thickness and leaching of H_3PO_4. In 2013, the same group (Oono et al., 2013) studied the long-term available operational duration of the HT-PEM fuel cells using H_3PO_4-doped, chemically cross-linked poly (2,5-benzimidazole) (ABPBI) membranes instead of PBI/H_3PO_4 membranes. Their research indicated that the available operational duration of the ABPBI membrane was longer than that of a PBI membrane. The thickness of the ABPBI membrane did not change significantly. In addition, the amount of Pt in the catalyst layer did not change. Park et al. (2020) studied the degradation phenomena and performance recovery of an HT-PEM fuel cell with a PBI/H_3PO_4 MEA. In this research, the relationship between cell degradation, exposed humidity and membrane H_3PO_4 loading was investigated. A 74.1% performance degradation was observed if the membrane was exposed to a humid environment. In addition, doping little H_3PO_4 in the electrodes recovered the cell performance. Li et al. (2021) studied the degradation phenomena of an HT-PEM fuel cell under a 600-h accelerated stress test. This study indicated that the activation polarization was the key issue which caused the performance degradation. In this research, a serious acid loss from the membrane after a load cycling test was as well observed.

Although the above studies showed some performance deterioration mechanisms of HT-PEM fuel cells, these studies were carried out with graphite BPs. The research about the deterioration phenomena of HT-PEM fuel cells using metal BPs is currently still rare. Therefore, for the future development of the HT- PEM fuel cells using metal BPs, understanding the deterioration phenomena of the HT-PEM fuel cells using bare stainless steel BPs is selected as the target in this research. The previous paper carried out by Yan et al. (2019) presented the performance deterioration rates of the HT-PEM fuel cells using different types of BP. To further understand the difference between the anodic and cathodic BPs after operation, the comparison between the anodic and cathodic BPs after a continuous operation are as well carried out in this work.

FUEL CELL AND EXPERIMENTAL SETUP

To study the performance deterioration phenomena of the HT-PEM fuel cell using bare stainless steel BPs, the performance of the fuel cell was continuously measured. The electrochemical impedance spectroscopy (EIS) technique was utilized for quantifying the resistance change of the HT-PEM fuel cell before and after operation. The morphology and element composition on the surface of the BPs after operation was as well investigated to understand the deterioration phenomena on the SS304 BP surface.

The HT-PEM Fuel Cell Using SS304 BPs

To carry out the continuous operation test for this research, a single HT-PEM fuel cell using the stamped SS304 BPs was assembled. The single cell comprises two terminal plates made of Al6061, two current collectors made of gold plating copper, two BPs made of uncoated 304 stainless steel, and a 25-cm^2 MEA.

The steel sheet for the stamped BPs was 0.2 mm thick. Two Z-shape flow channels were formed on the BP via a stamping process. Each single flow channel had a depth of 0.6 mm and a width of 1.3 mm. The distance between the two flow channels was 0.6 mm. The summed thickness of the metal sheet and the flow channel depth, *i.e,* the total thickness of the BP, was 0.8 mm. To prevent gas leaks, two gasket layers were installed on the stamped SS304 BPs. The detailed information of gaskets can be found in the previous paper (Chen et al., 2018). The assembly torque was 6 N-m. The model number of the MEA used in this study was AAM-25, a product from Advent Technologies Inc. The membrane in the MEA was an Advent TPS® membrane and was doped with H_3PO_4. The membrane had a pyridine-type structure and was PBI-free. Pt/C was selected as the catalyst material on the electrodes. Figure 1 shows the photos of the assembled HT-PEM fuel cell and the stamped uncoated SS304 BP used in this fuel cell.

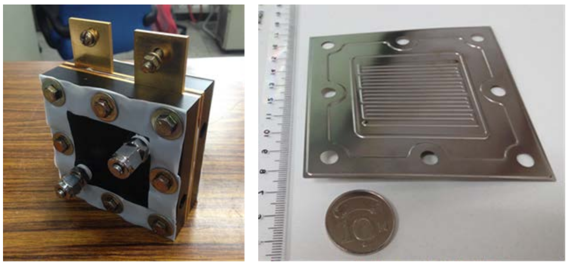
(a) (b)

Fig. 1. (a) The photo of the HT- PEM fuel cell using stamped SS304 BPs and (b) the photo of the stamped SS304 BP

Experimental Setup

To carry out the long-term duration tests of the HT-PEM fuel cell using SS304 BPs, a test facility with a continuous operation function (figure 2) was used to measure the continuous voltage and current data of the fuel cell. This test facility comprised a power measurement sub-system, a hydrogen and air supply sub-system, two gas bubbling-type humidifiers, a thermal management unit and a data logging unit. The highest current and voltage for the fuel cell test facility were 60 A and 60 V, respectively. The accuracy of all gas mass flow controllers in this experiment was ± 0.3% F.S.. To operate continuously, several sensors, including voltage sensors, temperature sensors and pressure sensors, were used to monitor the status of the fuel cell. To obtain the electrochemical impedance spectroscopy, an EIS measurement facility (brand : AMETEK®, model number: VersaSTAT4) was used to evaluate the impedance of the HT- PEM fuel cell at different operating time. To perform the EIS tests, a fixed direct current was pulled from the fuel cell. The impedance of the fuel cell was obtained by alternating the current under a periodic change with a frequency ranging from 10000 Hz to 0.01 Hz. The amplitude of the exciting current was 5% to 10% of the output direct current. To observe the surface morphology of the SS304 surface, a scanning electron microscope (SEM) supplied by Carl Zeiss Microscopy (model : JEOL JSM-6500F) was utilized in this paper. The energy-dispersive X-ray (EDX) spectroscopies of the bipolar plate samples were as well measured by the SEM to analyze surface element composition on the SS304 surface.

In the continuous operation and the EIS tests, the temperature of the fuel cell was fixed. In order to control the operating temperature of the HT-PEM fuel cell in this study, four high-power heating rods were inserted in the end plates, and a T-type thermocouple was inserted in the bipolar plate. A temperature controller was used to acquire the voltage signal from the thermocouple and to control the power supplied to heating rods. By controlling the power supplied to the heating rods and by covering the fuel cell with a heat insulation jacket, the operating temperature of the cell was maintained at 160±1.5°C. Hydrogen and air were flowed into the fuel cell with no humidification processes. The stoichiometric ratios of anodic (H_2) and cathodic (air) gases were set at 1.2 and 2.0, respectively. Prior to the performance measurement, the HT- PEM fuel cell was operated at 5 A for 24 h to complete the break-in process. During the formal cell continuous experiment, the output current was set at 5 A (200 mA cm^{-2}) within the first 50 h and was set at 7.5 A (300 mA cm^{-2}) after the 50th hour of deterioration experiment.

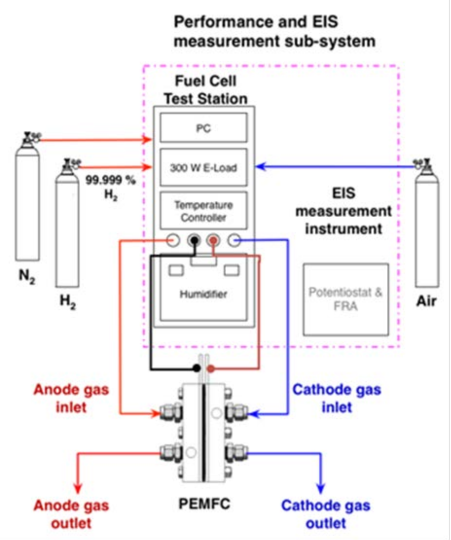

Fig. 2. The schematic diagram of the experimental setup for the deterioration test of the HT-PEM fuel cells using bare SS304 BPs

RESULTS AND DISCUSSION

In this research, the polarization curves and electrochemical impedance of the HT-PEM fuel cell with SS304 BPs at various operating hours were measured and recorded. The SEM images and surface element analysis results of the anodic and cathodic BPs of the HT-PEM fuel cell were shown and compared. To further understand the reasons for the difference of the surface condition between the anodic and cathodic BPs after operation, the phosphorus mapping of the MEA cross-section was as well captured.

Deterioration of Cell Performance

Figure 3 discloses the polarization curves of the tested HT-PEM fuel cell at different operating hours. As can be seen, the maximum cell power density is about 245.8 mW cm^{-2} and its corresponding cell voltage is 0.37 V at the 24th hour. However, the maximum power density drops to 160.1 mW cm^{-2} and 114.4 mW cm^{-2} at the 168th and the 384th hours, respectively. It is observed obviously that the output power of the HT-PEM fuel cell using bare SS304 BPs decreases along with the operating duration. The maximum power density drops by about 53.5% after a continuous 384-h operation. In the EIS test (figure 4), it is also found that the resistance of the fuel cell deteriorates with time. The total resistance of the fuel cell, a sum of ohmic resistance, activation resistance and mass transport resistance, can be obtained from the larger intercept on the x axis in an electrochemical impedance spectroscopy. As shown in Fig.4, the total resistance of the fuel cell, the intercept on the x axis at an EIS frequency of about 10-2 Hz, is about 748 mΩ cm^2 at the 24th hour and becomes 1440 mΩ cm^2 at the 384th hour. The total resistance of the fuel cell increases by about 92.5% after a 384-h continuous operation. From the EIS results, it is seen that not only the ohmic resistance (the smaller intercept on the x axis), but also the activation and mass transport resistance (the diameter of the arc) increases with operating duration. The increase in the arc diameter can be attributed to some reasons, including the physical deterioration of electrodes, the contamination of catalyst by phosphoric acid and the deterioration of the hydrophobicity of gas diffusion layer (GDL). The elevation of the ohmic resistance is inferred to be associated with loss of H_3PO_4 from the proton exchange membrane, and the increase in the electrical resistance of the BPs due to formation of a passivation film on the SS304 BP surface. Figure 5 exhibits the SEM images of the anodic SS304 BP after a 432 h continuous operation at 200, 500 and 2500 magnifications. From this figure, a rugged surface can be noted on the used SS304 plate surface. It is inferred that the rugged surface area is covered by a layer of passivation film caused by the oxidation and corrosion reactions on the metal surface. By contrast, the flat surface in the figure is the original SS304 surface which has not been corroded or oxidized yet.

In the previous study carried out by Yan et al. (2019), the surface morphology of the cathodic SS304 plate was examined and its surface elements were analyzed. It was inferred that the passivation film on the SS304 BP surface after a continuous operation was a layer of iron phosphate and ferric oxide caused by the oxidation and corrosion reactions. In this work, in addition to observing the microscopic surface image of the anodic BP of the HT-PEM fuel cell, understanding the difference between the anodic BP and the cathodic BP after a continuous operation is one of the major objectives as well. As a result, comparison of the anodic and cathodic BPs after a continuous operation is discussed in the next section.

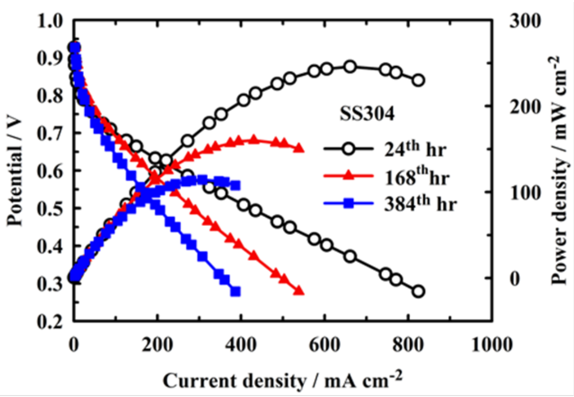

Fig. 3. The IV curves of the HT-PEM fuel cell using bare SS304 BPs at various operational time

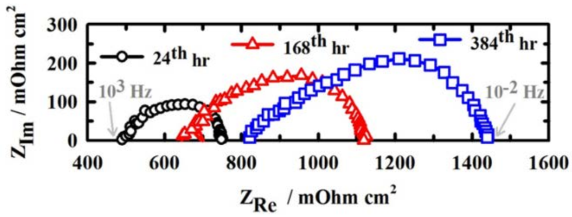

Fig. 4. The EIS results of the HT-PEM fuel cell using bare SS304 BPs at various operational time at 400 mA cm^{-2}

Comparison of The Anodic and Cathodic BPs After Operation

From Fig. 5, it is observed that the passivation film appears light or grey color, and the uncorroded surface appears dark color in the SEM images. To understand the difference of the corrosion levels on the anodic and cathodic BP surfaces, the SEM images of the unused SS304 BP, used anodic SS304 BP and the used cathodic SS304 BP at a 200 magnification are compared in figure 6. As can be seen in Fig.6, the BP surface after operation becomes more cratered than before operation. Moreover, the cathodic BP shows more light color areas than the anodic BP. These indicate that the passivation film is more widely distributed on the cathodic bipolar surface, implying a more serious oxidation or corrosion reaction on the cathode side.

To further examine the composition of the passivation film and to study the difference between the anodic and cathodic BPs after a continuous operation, the surface mapping of Fe, O and P elements on the anodic and cathodic BPs at a 2500 magnification was captured. The mapping results are disclosed in figure 7. From Fig.7(a), it is obviously observed that the O and P elements are concentrated in the rugged area on the anodic BP. However, the Fe element is uniformly distributed over the entire region. This result verifies the inference of that the rugged surface area in Fig.5 is covered by a layer of passivation film. In contrast to the anodic BP, the O and P elements distribution over the entire region on the cathodic BP (Fig.7(b)) are less concentrated. This is because the passivation film on the cathodic BP is more widely distributed due to more serious oxidation and corrosion reactions. Because of the existence of Fe, O and P elements on the SS304 BPs after a continuous operation, it is reasonable to infer that the passivation film is a mixed layer of iron phosphate and ferric oxide. According to Eqs. (1)-(2), formation of ferric oxide on the steel surface can be attributed to the existence of H_2O which is produced due to the H_2 oxidation reaction in the fuel cell. In addition, because of the existence of phosphoric acid in the polymer membrane and the acid leak phenomenon, iron phosphate is expected to be formed according to Eq. (3).

$$Fe + H_2O \rightarrow FeO + 2H^+ + 2e^-. \qquad (1)$$

$$2FeO + H_2O \rightarrow Fe_2O_3 + 2H^+ + 2e^-. \qquad (2)$$

$$Fe_2O_3 + 2H_3PO_4 \rightarrow 2FePO_4 + 3H_2O. \qquad (3)$$

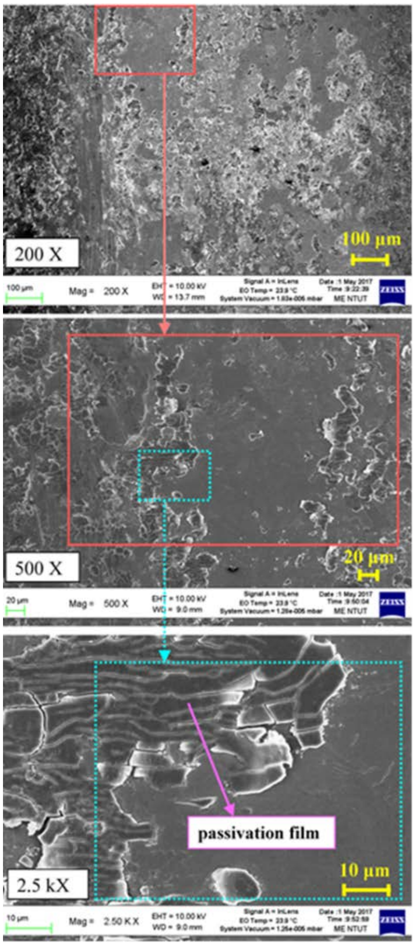

Fig. 5. The SEM images of the anodic SS304 BP after a 432-hr continuous operation at 200, 500 and 2500 magnifications

The products of the oxidation and corrosion reactions reduce the electrical resistance of the SS304 BP because these compounds have lower electrical conductivity. Furthermore, the rugged surface resulted from the formation of the compounds leads to a higher contact resistance between the BPs and the GDLs. Owing to the above two reasons, the electron transport resistance of the SS304 BP increases after a continuous operation, which is one of the reasons for the deterioration of the cell performance. Water is produced on the cathode side according to the working mechanism of a PEM fuel cell. Although some water diffuses from cathode to anode due to a concentration difference, the amount of water on the cathode side is still more than the anode side. In addition, the amount of leaked phosphoric acid on the cathode side is more than the anode side because the attractive force between water and acid drags phosphoric acid moving to the cathode side. Thus, the oxidation and corrosion reactions on the cathode are more serious, leading to a more widely distributed O and P elements on the cathodic BP is. To verify that there is more phosphoric acid leaking on the cathode side, the phosphorus mapping on the cross section of a used MEA is further captured. The result is presented and discussed in the latter part of this article.

To further verify the above discussion about Fig.6 and Fig.7, a quantitative surface element analysis of the unused SS304 plate and used anodic SS304 BP by the EDX approach was carried out. Figure 8(a) and Fig.8(b) present the scanned areas and the EDX spectroscopies of an unused SS304 plate and a used anodic SS304 BP sample after a 432-h continuous operation, respectively. To compare the surface element compositions of the unused, used anodic and used cathodic BPs, the EDX result of the cathodic BP in the previous paper carried out by Yan et al. (2019) is cited in this paper. In this work, the C, O, P and Fe elements are the studied targets because C and Fe are two major elements of SS304, and because the surface oxidation and corrosion reactions are expected to lead to an elevation of the amount of O and P elements on the plate surface. Figure 9 shows the comparison of the EDX results of the three different BPs. As disclosed in Fig.9, the atomic concentrations of the C and Fe elements on the both anodic and cathodic BPs decrease after a continuous operation. The change of Fe element is especially significant because the Fe element is an active reductant and thus its concentration becomes much smaller as a corrosion or oxidation reaction occurs upon on the Fe element. The dramatic increase in the O and P elements can also be seen in Fig.9. These results verify that the SS304 BPs in the high temperature PEM fuel cell suffer from serious oxidation and corrosion problems. It is also observed that the atomic concentration of P element is almost 0% on the unused SS304 plate, but it becomes 4.6% and 7.1 % on the used anodic and used cathodic BPs, respectively. Since the only phosphorus source in the high temperature PEM fuel cell is H_3PO_4 in the proton exchange membrane, it can be confirmed that H_3PO_4 leaking from the membrane during the fuel cell operation is the major cause for formation of phosphorus related compound on the BP surface. It can be also found that the element concentrations on the used anodic BP are close to that on the used cathodic BP except for the P element. The atomic concentration of P element on the cathodic BP is 54.3% higher than that on the anodic BP. This result reflects the inference of more H_3PO_4 leaks on the cathode side in the discussion about Fig.7.

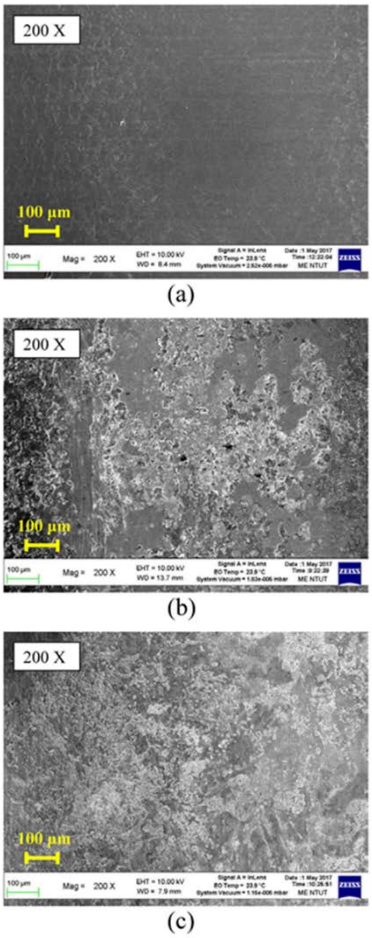

(a)

(b)

(c)

Fig. 6. The SEM images of (a) the unused SS304 BP, (b) the anodic BP after operation, and (c) the cathodic BP after operation at a 200 magnification

To obtain a direct evidence of more H_3PO_4 leaks on the cathode side, the phosphorus EDS mapping on the cross sections of the unused and used H_3PO_4 doped MEAs is captured and the results are revealed in figure 10. As shown in Fig.10, the P element is concentrated in the membrane and catalyst regions before the cell operation. However, the P element distribution on the used MEA becomes less concentrated. Apparently, the amount of P element in the GDL becomes more after operation. It is as well observed that the amount of detected P element on the cathode GDL is more than that on the anode side. These results provide an evidence of more phosphoric acid leaks on the cathode side, which leads to a more serious corrosion problem and a wider rugged surface area on the cathodic SS304 BP.

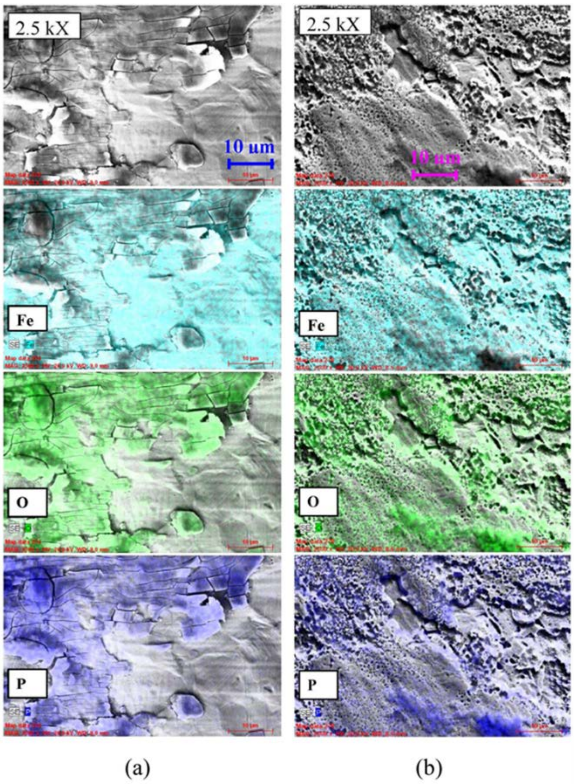

(a) (b)

Fig. 7. The EDS mapping results of (a) the anodic surface and (b) the cathode side of the SS304 BP after 432 hour operation at a 2500 magnification

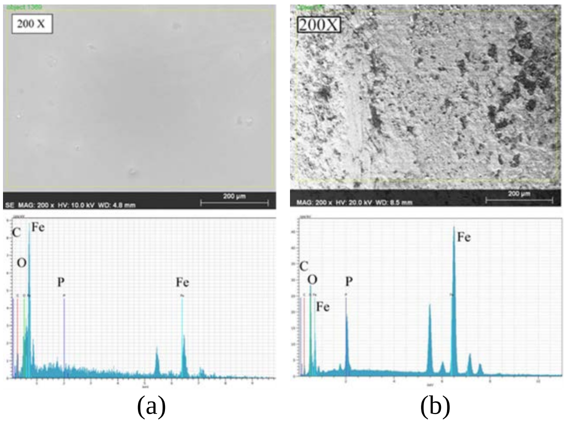

(a) (b)

Fig. 8. The EDX spectroscopies of (a) the unused SS304 BP and (b) the used anodic SS304 BP

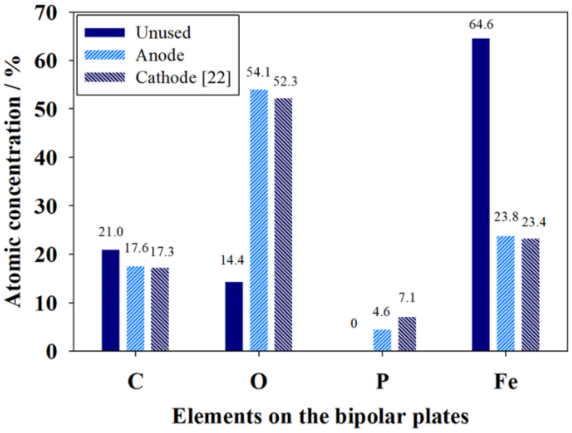

Fig. 9. The EDX results of the unused, used anodic and used cathodic BPs

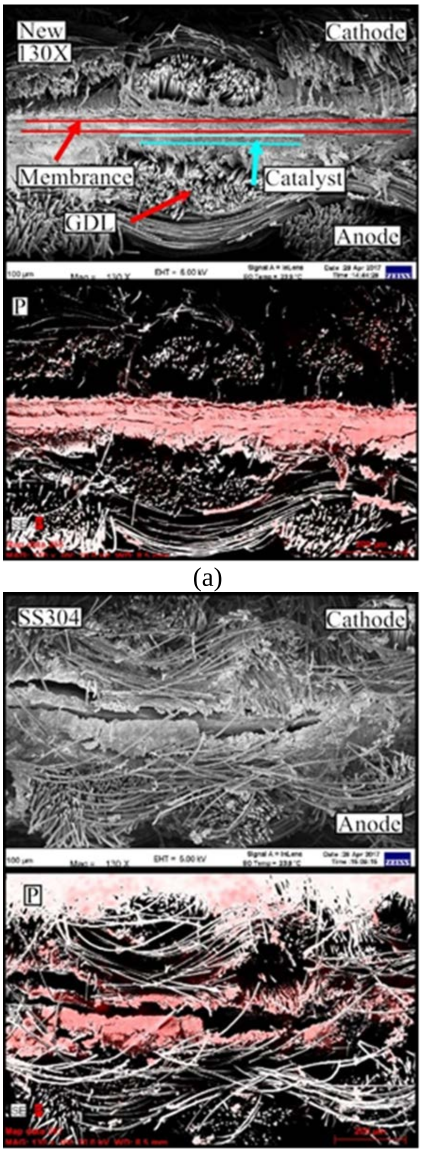

(a)

(b)

Fig. 10. The phosphorus EDS mapping results on the cross sections of (a) the fresh H3PO4–contained MEA and ; (b) the H3PO4–contained MEA after a 432 hour operation

CONCLUSIONS

The deterioration phenomena of the HT-PEM fuel cell using bare SS304 bipolar plates are investigated in this research. The output power of the HT-PEM fuel cell decreases with operating duration. The maximum power density of the HT-PEM fuel cell drops by about 53.5% after a continuous 384-h operation. In addition, the total fuel cell resistance increases by about 92.5% after the continuous operation. One of the major reasons for the deterioration of the cell performance and the raise of the total cell resistance is the increase in the electrical resistance of the bipolar plates due to formation of passivation film on the SS304 bipolar plate surface, which is caused by the oxidation and corrosion reactions on the metal surface. The cathodic bipolar plate after a continuous operation has a larger rugged surface area and a wider O and P elements distribution than the anodic bipolar plate, because of more produced water and more H_3PO_4 leaks on the cathode side of the HT-PEM fuel cell. The research results indicate that the cathodic SS304 bipolar plate may suffer from more serious oxidation and corrosion problems in the HT-PEM fuel cell. As a result, a stricter anti-corrosion criterion for the cathodic bipolar plate may be needed when considering the anti-corrosion approaches for the metal bipolar plates in HT-PEM fuel cells.

ACKNOWLEDGMENT

The authors appreciate the financial support from the Ministry of Science and Technology (MOST), Taiwan, under the grant number of MOST 109-3116-F-006-014-CC1 and MOST 109-2221-E-415-007-MY3.

REFERENCES

Altaf, F., Batool, R., Gill, R., Rehman, Z.U., Majeed, H., Ahmad, A., Shafiq, M., Dastan,D., Abbas, G., Jacob, K., “Synthesis and electrochemical investigations of ABPBI grafted montmorillonite based polymer electrolyte membranes for PEMFC applications,”; Renew. Energy, Vol.164, pp.709-728(2021).

Charalampopoulos, C., Kallitsis, K.J., Anastasopoulos, C., Daletou, M.K., Neophytides, S.G., Andreopoulou, A.K., Kallitsis, J.K., “Crosslinked polymer electrolytes of high pyridine contents for HT-PEM fuel cells,”; Int. J. Hydrogen Energy, Vol.45, No.60, pp.35053-35063(2020).

Chen, H., Wang, S., Liu, F., Wang, D., Li, J., Mao, T., Liu, G., Wang, X., Xu, J., Wang, Z., “Base-acid doped polybenzimidazole with high phosphoric acid retention for HT-PEMFC applications,”; J. Membr. Sci., Vol.596, pp.117722 (9 pages)(2020).

Chen, C.Y., Su, S.C., “Development and performance evaluation of a high temperature proton exchange membrane fuel cell with stamped 304 stainless steel bipolar plates,” ; Int. J. Hydrogen Energy, Vol.43, No.29, pp.13430-13439(2018).

Eveloy, V., Gebreegziabher, T., “A review of projected power-to-gas deployment scenarios,”; Energies, Vol.11, No.7, pp.1824 (52 pages)(2018).

Gondal, I.A., “Hydrogen integration in power-to-gas networks,”; Int. J. Hydrogen Energy, Vol.44, No.3, pp.1803-1815(2019).

González-Gutiérrez, A.G., Pech-Canul, M.A., Chan-Rosado, G., Sebastian, P.J., “Studies on the physical and electrochemical properties of Ni-P coating on commercial aluminum as bipolar plate in PEMFC,”; Fuel, Vol.235, pp.1361-1367(2019).

Hu, R., Tang, J., Zhu, G., Deng, Q., Lu, J., “The effect of duty cycle and bias voltage for graphite-like carbon film coated 304 stainless steel as metallic bipolar plate,”; J. Alloys Compd., Vol.772, pp.1067-1078(2019).

Hu, J., Zhang, H., Zhai, Y., Liu, G., Hu, J., Yi, B., “Performance degradation studies on PBI/H3PO4 high temperature PEMFC and one-dimensional numerical analysis,”; Electrochim. Acta, Vol.52, No.2, pp.394-401(2006).

Hu, J., Zhang, H., Zhai, Y., Liu, G., Hu, J., Yi, B., “500 h Continuous aging life test on PBI/H3PO4 high-temperature PEMFC,” ; Int. J. Hydrogen Energy, Vol.31, No.13, pp.1855-1862(2006).

Liu, G., Zhang, H., Hu, J., Zhai, Y., Xu, D., Shao, Z., “Studies of performance degradation of a high temperature PEMFC based on H3PO4-doped PBI,”; J. Power Sources, Vol.162, No.1, pp.547-552(2006).

Li, J., Yang, L., Wang, Z., Sun, H., Sun, G., “Degradation study of high temperature proton exchange membrane fuel cell under start/stop and load cycling conditions,” ; Int. J. Hydrogen Energy, Vol.46, No.47, pp.24353-24365(2021).

Moreno, N.G., Molina, M.C., Gervasio D., Pérez Robles, J.F., “Approaches to polymer electrolyte membrane fuel cells (PEMFCs) and their cost,”; Renew. Sust. Energy Rev., Vol.52, pp.897-906(2015).

Modestov, A.D., Tarasevich, M.R., Filimonov, V.Ya, Zagudaeva, N.M., “Degradation of high temperature MEA with PBI-H3PO4 membrane in a life test,”; Electrochim. Acta, Vol.54, No.27, pp.7121-7127(2009).

Oono, Y., Fukuda, T., Sounai, A., Hori, M., “Influence of operating temperature on cell performance and endurance of high temperature proton exchange membrane fuel cells,”; J. Power Sources, Vol.195, No.4, pp.1007-1014(2010).

Oono, Y., Sounai, A., Hori, M., “Long-term cell degradation mechanism in high-temperature proton exchange membrane fuel cells,” ; J. Power Sources, Vol.210, pp.366-373(2012).

Oono, Y., Sounai, A., Hori, M., “Prolongation of lifetime of high temperature proton exchange membrane fuel cells,” ; J. Power Sources, Vol.241, pp.87-93(2013).

Park, H., Kim, H., Kim, D.K., Lee, W.J., Choi, I., Kim, H.J., Kim, S.K., “Performance deterioration and recovery in high-temperature polymer electrolyte membrane fuel cells: Effects of deliquescence of phosphoric acid,”; Int. J. Hydrogen Energy, Vol.45, No.57, pp.32844-32855(2020).

Qi, Z., Buelte, S., “Effect of open circuit voltage on performance and degradation of high temperature PBI–H3PO4 fuel cells,”; J. Power Sources, Vol.161, No.2, pp.1126-1132(2006).

Song, Y., Zhang, C., Ling, C.Y., Han, M,. Yong, R.Y., Sun, D., Chen, J., “Review on current research of materials, fabrication and application for bipolar plate in proton exchange membrane fuel cell,”; Int. J. Hydrogen Energy, Vol. 45, No.54, pp.29832-29847(2020).

Shi, J., Zhang, P., Han, Y., Wang, X., Yu, Y., Sun, J., “Investigation on electrochemical behavior and surface conductivity of titanium carbide modified Ti bipolar plate of PEMFC,”; Int. J. Hydrogen Energy, Vol.45, No.16, pp.10050-10058(2020).

Yusoff, Y.N., Loh, K.S., Wong, W.Y., Daud, W.R.W., Lee, T.K., “Sulfonated graphene oxide as an inorganic filler in promoting the properties of a polybenzimidazole membrane as a high temperature proton exchange membrane,”; Int. J. Hydrogen Energy, Vol.45, No.51, pp.27510-27526(2020).

Yan, W.M., Chen, C.Y., Liang, C.H., “Comparison of performance degradation of high temperature PEM fuel cells with different bipolar plates,” ; Energy, Vol.186, pp.115836 (9 pages)(2019).

ABBREVIATIONS

BPs	bipolar plates
EDX	energy-dispersive X-ray
EIS	electrochemical impedance spectroscopy
GDL	gas diffusion layer
HT-PEM	high temperature proton exchange membrane
MEA	membrane electrode assembly
ABPBI	poly(2,5-benzimidazole)
PEM	proton exchange membrane
SEM	scanning electron microscope

無鍍層不銹鋼雙極板高溫型質子交換膜燃料電池之衰退現象

陳震宇
國立嘉義大學機械與能源工程學系

梁家豪
國立臺北科技大學能源與冷凍空調工程系

摘要

金屬雙極板高溫型質子交換膜燃料電池可解決目前傳統質子交換膜燃料電池CO容忍度太低及雙極板成本太高的問題，而為了進一步增加此型燃料電池之壽命，必須先了解在金屬雙極板未鍍膜情況下，電池的性能衰退現象，也因此，本研究之目的乃探討且驗證此型燃料電池之基礎性能衰退現象。實驗結果顯示使用未鍍膜304不銹鋼雙極板電池在經過384小時連續操作後，功率下降53.5%，而電池總阻抗增加92.5%，而電池性能衰退的主要原因則是因為在不銹鋼雙極板表面上所發生的氧化及腐蝕現象會形成一層鈍化層，此一鈍化層會進一步導致雙極板之導電阻抗上升。另外，在長時間操作後，觀察陰陽極之雙極板表面型態，可發現陰極雙極板表面較為崎嶇，其表面氧及磷元素之分佈亦較廣，推測此乃因陰極側有較多反應產生的水及從質子交換膜滲出的磷酸，因此在陰極側有著較劇烈的腐蝕及氧化反應，也因此，對使用金屬雙極板的高溫型質子交換膜燃料電池而言，陰極金屬雙極板需要更高的抗腐蝕標準。